Published OnlineFirst February 14, 2018; DOI: 10.1158/1535-7163.MCT-17-0552

Cancer Biology and Translational Studies

Molecular Cancer Therapeutics

Molecular Pharmacodynamics-Guided Scheduling of Biologically Effective Doses: A Drug Development Paradigm Applied to MET Tyrosine Kinase Inhibitors

Apurva K. Srivastava[1], Melinda G. Hollingshead[2], Jeevan Prasaad Govindharajulu[1], Joseph M. Covey[3], Dane Liston[3], Melanie A. Simpson[1], James O. Peggins[3], Donald P. Bottaro[4], John J. Wright[3], Robert J. Kinders[1], James H. Doroshow[3,5], and Ralph E. Parchment[1]

Abstract

The development of molecularly targeted agents has benefited from use of pharmacodynamic markers to identify "biologically effective doses" (BED) below MTDs, yet this knowledge remains underutilized in selecting dosage regimens and in comparing the effectiveness of targeted agents within a class. We sought to establish preclinical proof-of-concept for such pharmacodynamics-based BED regimens and effectiveness comparisons using MET kinase small-molecule inhibitors. Utilizing pharmacodynamic biomarker measurements of MET signaling (tumor $pY^{1234/1235}$MET/total MET ratio) in a phase 0–like preclinical setting, we developed optimal dosage regimens for several MET kinase inhibitors and compared their antitumor efficacy in a *MET*-amplified gastric cancer xenograft model (SNU-5). Reductions in tumor $pY^{1234/1235}$MET/total MET of 95%–99% were achievable with tolerable doses of EMD1214063/MSC2156119J (tepotinib), XL184 (cabozantinib), and XL880/GSK1363089 (foretinib), but not ARQ197 (tivantinib), which did not alter the pharmacodynamic biomarker. Duration of kinase suppression and rate of kinase recovery were specific to each agent, emphasizing the importance of developing customized dosage regimens to achieve continuous suppression of the pharmacodynamic biomarker at the required level (here, ≥90% MET kinase suppression). The customized dosage regimen of each inhibitor yielded substantial and sustained tumor regression; the equivalent effectiveness of customized dosage regimens that achieve the same level of continuous molecular target control represents preclinical proof-of-concept and illustrates the importance of proper scheduling of targeted agent BEDs. Pharmacodynamics-guided biologically effective dosage regimens (PD-BEDR) potentially offer a superior alternative to pharmacokinetic guidance (e.g., drug concentrations in surrogate tissues) for developing and making head-to-head comparisons of targeted agents. *Mol Cancer Ther; 17(3); 698–709. ©2018 AACR.*

Introduction

Maximum tolerable dose (MTD)-based anticancer regimens, originally developed for radiation and cytotoxic chemotherapy, are inappropriate for many modern, targeted oncology therapies. MTD-based regimens can result in toxicity-related issues, including trial discontinuations, low patient adherence, and enhanced toxicities in combination therapies (1, 2), as well as unnecessary drug costs, given that increased drug concentrations do not always increase tumor exposure or response (2–4). Biologically effective dose (BED)-based cancer therapy can address these issues through administration of the lowest dose required to achieve adequate suppression of the molecular driver of tumor growth. Critical to establishing BED-based regimens is selecting a dosing schedule sufficient to sustain target inhibition between doses, thereby maximizing effectiveness by eliminating intervals of target function recovery (3). This is analogous to the microbiology concept of the minimum inhibitory concentration (MIC) of beta-lactams required to suppress microbial growth (5). Defining such biologically effective dosage regimens (BEDR) for multiple agents that target the same molecule or pathway but differ structurally and/or pharmacologically will facilitate head-to-head comparison, as single agents or in combination with additional drugs, in preclinical models or patients; different targeted agents may yield equivalent efficacy when they achieve equivalent control of the molecular target(s) that drive a specific malignancy.

[1]Clinical Pharmacodynamics Biomarker Program, Applied/Developmental Research Directorate, Leidos Biomedical Research, Inc., Frederick National Laboratory for Cancer Research, Frederick, Maryland. [2]Biological Testing Branch, Developmental Therapeutics Program, Frederick National Laboratory for Cancer Research, Frederick, Maryland. [3]Division of Cancer Treatment and Diagnosis, National Cancer Institute, Bethesda, Maryland. [4]Urologic Oncology Branch, National Cancer Institute, Bethesda, Maryland. [5]Center for Cancer Research, National Cancer Institute, Bethesda, Maryland.

Note: Supplementary data for this article are available at Molecular Cancer Therapeutics Online (http://mct.aacrjournals.org/).

Corresponding Author: Ralph E. Parchment, Clinical Pharmacodynamics Biomarker Program, Applied/Developmental Research Directorate, Leidos Biomedical Research, Inc., Frederick National Laboratory for Cancer Research, PO Box B, Frederick, MD 21702. Phone: 301-846-6630; Fax: 301-846-6651; E-mail: parchmentr@mail.nih.gov

doi: 10.1158/1535-7163.MCT-17-0552

Published OnlineFirst February 14, 2018; DOI: 10.1158/1535-7163.MCT-17-0552

BEDR determination may begin in preclinical studies but is readily translatable to a clinical setting. Defining a BEDR requires a mechanism of action related to preclinical and/or clinical efficacy as well as pharmacodynamic biomarkers for measuring that mechanism of action to examine the extent and duration of target response. Preclinical pharmacodynamic biomarker studies enable delineation of the degree of target inhibition associated with antitumor efficacy. Subsequently, a clinical phase 0 trial, which has no therapeutic intent, but instead aims to obtain pharmacologic data from a limited number of patients (6), may be used to investigate the dose and schedule that maintain this desired level of target inhibition in patients. For example, using a validated pharmacodynamic assay for PAR (poly[ADP-ribose]), the enzymatic product of PARP 1/2 (poly[ADP-ribose] polymerase 1/2) catalytic activity and a biomarker of PARP inhibitor action, a phase 0 trial of veliparib established a twice-daily dosage regimen that prevented full recovery of PAR between doses (7), and this regimen has been used subsequently for clinical development of combination therapies (3, 8–10). A phase 0 setting may also be used to make head-to-head comparisons among two or more agents targeting the same pathway or molecule, thereby enabling selection of a single agent for phase I testing.

Eighteen small-molecule targeted inhibitors of the receptor tyrosine kinase MET (hepatocyte growth factor receptor) have been tested in the clinic, and MET signaling is integral to progression, metastasis, and therapeutic resistance in several types of cancer (11). Several MET signaling inhibitors are FDA-approved cancer therapies or are in late-stage development, and the majority of these suppress phosphorylation of specific tyrosine residues, notably pY^{1234}, pY^{1235}, pY^{1349}, and pY^{1356}, that are critical for kinase activity and signal transduction (12–15). Although there are no generally accepted criteria to empirically link suppression of phosphorylated MET (pMET) to antitumor efficacy, a decrease in the proportion of MET phosphorylated at $pY^{1234/1235}$ relative to total full-length MET (the $pY^{1234/1235}$MET to total MET ratio, herein referred to as "$pY^{1234/1235}$MET/MET") has been validated as a pharmacodynamic biomarker of MET kinase inhibition, following our recent development of immunoassays for both the total full-length and dually $pY^{1234/1235}$-phosphorylated MET species (16).

A direct comparison of the efficacies of MET tyrosine kinase inhibitors (TKIs) from different chemical families and with distinct kinase inhibition profiles could inform selection of optimal treatment (dose, schedule, and drug) for patients with MET-driven cancers. A pharmacodynamically guided approach to assess antitumor efficacy at a specific degree of target inhibition is clinically relevant because it reflects the mechanism of target-driven activity in tumor tissue. For example, preclinical studies of the dual MET/ALK inhibitor crizotinib (17, 18) identified levels of pMET and pALK suppression (and corresponding plasma drug concentrations) associated with tumor growth inhibition in xenograft models, and the resulting pharmacokinetic-pharmacodynamic model was used to retrospectively determine that the recommended phase II dose, which produced clinical responses in ALK-positive NSCLC patients, likely yields pMET and pALK suppression levels similar to those required for antitumor activity in their preclinical studies (19). However, despite these results highlighting the promise of a pharmacodynamics-guided approach, dosage regimens for small-molecule MET TKIs, as for most targeted agents, have been established using MTDs (11, 20–23).

Here, we evaluate the pharmacodynamic effects of the ATP-competitive MET TKIs XL880 (20, 24), XL184 (25, 26), and EMD1214063 (27) and the putative allosteric MET inhibitor ARQ197 (ref. 21; Supplementary Fig. S1). We then apply these relationships to compare antitumor efficacies of these inhibitors when administered on customized dosing schedules predicted to continuously suppress $pY^{1234/1235}$MET/MET by 90%—a level that was selected on the basis of a study of PF02341066 (crizotinib) that equated > 90% transient pMET suppression with tumor growth inhibition, but not regression, in a *MET*-amplified preclinical model (17). Furthermore, by examining pharmacodynamic measurements from a small number of clinically feasible time points, we model how this pharmacodynamic biomarker endpoint could be used as a primary endpoint of a clinical phase 0 trial comparing depth and duration of the molecular response to safe single doses of several agents, with patient cohorts representing different time points after drug administration. Our results demonstrate the effectiveness of pharmacodynamics-guided, biologically effective dosage regimens in achieving sustained molecular target control and, thereby, antitumor efficacy, supporting proof-of-concept evaluation of this approach in the clinic.

Materials and Methods

Therapeutic agents

MET TKIs EMD1214063 (NSC 758244, tepotinib), ARQ197 (NSC 758242, tivantinib), XL184 (NSC 761068, cabozantinib), and XL880 (NSC 755775, GSK1363089, active ingredient in foretinib) were obtained from the Developmental Therapeutics Program, National Cancer Institute (NCI, Bethesda, MD). Chemical structures are shown in Supplementary Fig. S1. Agent purity was confirmed by proton–carbon NMR, high-performance liquid chromatography (HPLC), and mass spectrometry.

Animal models and drug administration

The Frederick National Laboratory for Cancer Research (FNLCR) is accredited by the Association for Assessment and Accreditation of Laboratory Animal Care International and follows the Public Health Service Policy for the Care and Use of Laboratory Animals. All studies were conducted according to an approved animal care and use committee protocol in accordance with procedures outlined in the "Guide for Care and Use of Laboratory Animals 8th Edition" (National Research Council; 2011; The National Academies Press; Washington, D.C.).

Female athymic nu/nu (NCr) mice (NCI Animal Production Program, Frederick, MD) were implanted subcutaneously with SNU-5 or GTL-16 human gastric tumor cells (16). Mice were housed in sterile, filter-capped, polycarbonate cages (Allentown Caging) maintained in a barrier facility on a 12-hour light/dark cycle and were provided sterilized food and water *ad libitum*. Mice were randomized into groups before initiation of treatment using a commercial software program (Study Director, Studylog Systems, Inc.).

Single-dose pharmacokinetic/pharmacodynamic study

After tumors reached 200 mm^3, mice were orally administered with MET inhibitor at doses equivalent to the human MTDs, as known at the time of study design (20, 28, 29), and 1/3, 1/6, and 1/10 MTD; as the MTD was unknown for EMD1214063 at the time of this study, we used doses that were shown in the literature

Published OnlineFirst February 14, 2018; DOI: 10.1158/1535-7163.MCT-17-0552

to be active (27, 30). Doses were EMD1214063 at 1, 3, 10, and 30 mg/kg; ARQ197 at 6, 24, 80, and 240 mg/kg; XL184 at 3.3, 5.5, 11, and 33 mg/kg; and XL880 at 8.3, 14, 28, and 83 mg/kg. Agents were prepared as follows: XL880, 0.75% hydroxypropyl methylcellulose (HPMC)/0.15% sodium lauryl sulfate (SLS) in distilled water; EMD1214063, 10% dimethyl sulfoxide (DMSO) in saline; XL184, distilled water; ARQ197, polyethylene glycol 400: 20% vitamin E-d-α tocopheryl polyethylene glycol 1000 succinate (TPGS) solution (60:40). Plasma and tumor samples ($n = 3$/time point) collected 0.5, 1, 2, 4, 6, 12, and 24 hours after drug administration were flash frozen for pharmacokinetic and pharmacodynamic analyses.

Multiple-dose pharmacodynamic-BEDR efficacy assessment

Mice were given oral doses of XL880 (17 mg/kg once daily), XL184 (44 mg/kg twice daily), or EMD1214063 (12.5 mg/kg twice daily) for 21 days once tumors reached 150 mm^3. These dosage regimens were selected based on pharmacodynamic data from the single-dose study; we used clinically relevant dose increment ratios of 1.33 or 1.2 to escalate from the dose level that had yielded slightly less than adequate $pY^{1234/1235}$MET/MET suppression in the single-dose study. Tumor volumes were recorded daily up to study day 62, and tumor growth inhibition was determined by percent treatment/control (%T/C; ref. 31).

Pharmacodynamics-based dosage regimen optimization for EMD1214063

For single-dose pharmacodynamic biomarker assessments, mice bearing GTL-16 or SNU-5 tumors were given a single dose of EMD1214063 (3.125, 12.5, 50, or 100 mg/kg) after tumors reached 150 mm^3. Tumor samples ($n = 6$/time point) were collected 4, 12, and 24 hours after drug administration and flash frozen for pharmacodynamic analyses. For the corresponding antitumor efficacy study in the SNU-5 model, oral doses of EMD1214063 (3.125, 12.5, or 50 mg/kg twice daily or 100 mg/kg once daily) were administered for 21 days once tumors reached 150 mm^3, and tumor volumes and animal body weights were recorded every 3–4 days up to study day 48.

Xenograft sample collection

Mice were anesthetized by isoflurane gas inhalation before tumor resection. Xenograft tumors were collected by standard dissection methods, cut into four equal pieces with fine-point scissors, and placed into screw-capped 1.5-mL Sarstedt cryovials (Nümbrecht) that were precooled in liquid nitrogen. All samples were frozen within one minute of excision and stored at −80°C until use. Specimen collection and handling conditions reflect those used at the NIH Clinical Center (Bethesda, MD) for patient samples (32, 33).

Multiple-dose pharmacodynamics study

Mice with SNU-5 tumors were treated with oral doses of XL880 (17 mg/kg once daily), XL184 (44 mg/kg twice daily), or EMD1214063 (12.5 mg/kg twice daily) each day for 8 days after tumors reached 150 mm^3. To profile the reversibility of MET kinase inhibition over 24 hours following the first and last doses, tumor samples were collected as described at 4, 12, and 24 hours after administration of the morning doses on treatment day 1 and day 8 (the scheduled afternoon doses of the EM1214063 and XL184 twice-daily regimens were withheld).

Pharmacodynamic biomarker assessment of MET kinase activity

Sandwich immunoassays for total and phosphorylated ($pY^{1234/1235}$) full-length MET in whole tumor cell lysates were developed and validated as described previously (16). These assay values were then used to calculate the pharmacodynamic biomarker of drug action, $pY^{1234/1235}$MET/MET. This ratio is a robust pharmacodynamic biomarker in preclinical models; importantly, it is not confounded by mouse cell infiltration into the SNU-5 human tumor xenografts (16). Samples were assayed in duplicate.

Analysis of plasma and tumor pharmacokinetics

Analytes were separated by reverse-phase HPLC and quantified by multiple-reaction monitoring using a triple-quadrupole mass spectrometer operating in the electrospray ionization, positive-ion mode. Standard criteria for acceptable accuracy and reproducibility were applied. Limits of quantitation ranged from 10 to 100 ng/mL.

Pharmacokinetic parameters were estimated from plasma or tumor concentration versus time data for each inhibitor using WinNonlin (Pharsight Corp.), Version 4.1 (ARQ197 and EMD-1214063), or Version 5.2 (XL184 and XL880), using noncompartmental models.

Statistical analysis

All descriptive statistics (including mean, SD, and CV), Student unpaired *t* test (two-tailed), and Fisher exact test were conducted using Microsoft Excel and GraphPad Prism software (v3.04). All tests were two-tailed with the statistical significance level (α) set to $P = 0.05$ (95% confidence level).

Results

Changes in $pY^{1234/1235}$MET/MET after single-dose administration

We titrated each of the 4 MET inhibitors to determine the minimal single dose and time required to inhibit MET phosphorylation by 90% (using the ratio of $pY^{1234/1235}$MET to total full-length MET as the pharmacodynamic biomarker) as well as the time course of $pY^{1234/1235}$MET/MET recovery following a single dose. Time course and duration of $pY^{1234/1235}$MET/MET suppression varied considerably among the inhibitors: ARQ197 failed to reduce $pY^{1234/1235}$MET (Fig. 1A) at any time point after drug administration, consistent with its recently demonstrated lack of MET TKI activity (16, 34, 35). EMD1214063 administered at the two highest doses (Fig. 1B) caused the most rapid 90% reduction in $pY^{1234/1235}$MET/MET (within 1 hour), with 90% suppression sustained through 12 hours. XL184 also caused a rapid $pY^{1234/1235}$MET reduction at the highest dose, but this targeted pharmacodynamic response was not appreciably sustained past the 6-hour collection point (Fig. 1C). XL880 required 2 hours to achieve a 90% reduction in $pY^{1234/1235}$MET/MET and showed the longest duration of molecular target suppression: out to 48 hours with the highest dose (Fig. 1D).

Preclinical modeling of a phase 0 study to develop customized, pharmacodynamics-based dosage regimens

To model the use of the $pY^{1234/1235}$MET/MET pharmacodynamic biomarker in selecting the dose and schedule of MET inhibitors in a clinical setting, we examined levels of this pharmacodynamic biomarker at different doses and at different

Published OnlineFirst February 14, 2018; DOI: 10.1158/1535-7163.MCT-17-0552

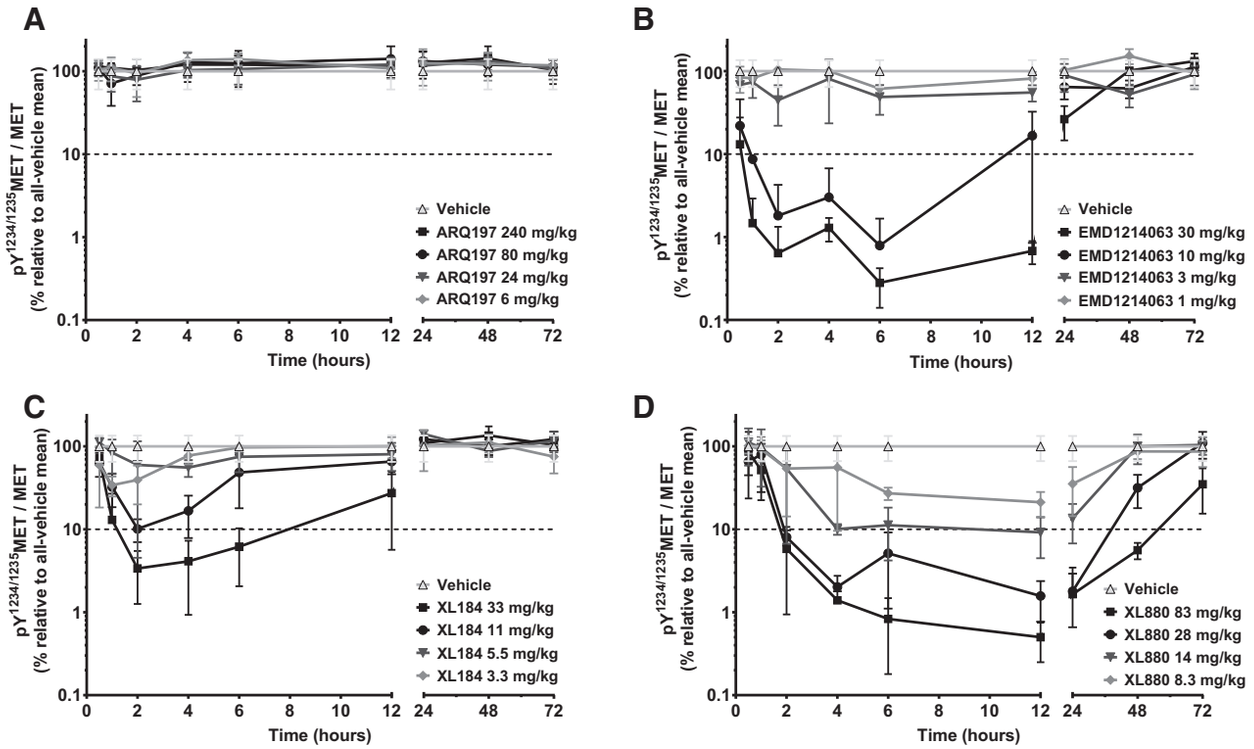

Figure 1.

Time course of MET kinase pharmacodynamic biomarker response ($pY^{1234/1235}$MET/MET reduction) to single-dose ARQ197 (**A**), EMD1214063 (**B**), XL184 (**C**), and XL880 (**D**) at increasing dose levels in the SNU-5 xenograft model. The *x*-axis indicates time after drug administration and is split for resolution. The log-scale *y*-axis indicates the mean pharmacodynamic biomarker value in each treated group relative to the all-vehicle mean (the 90% inhibition threshold is indicated by the dotted line). Error bars, SD ($n = 3$ animals per group).

clinically relevant time points, each of which would represent a different patient cohort in a phase 0 clinical study of pharmacodynamic responses to a single dose of each agent (Fig. 2). Examination of $pY^{1234/1235}$MET/MET at the 12- and 24-hour time points was critical for determining whether a daily (QD) or twice-daily (BID) schedule was required for sufficient duration of the ≥90% pharmacodynamic biomarker suppression; in the case of EMD1214063 and XL184 (Fig. 2A and B), the $pY^{1234/1235}$MET/MET recovery between 12 and 24 hours at even the highest doses tested necessitated twice-daily scheduling for these two agents. In contrast, the sustained ≥90% $pY^{1234/1235}$MET/MET suppression conferred by XL880 (Fig. 2C), which persisted even at 24-hours postdose, rendered a daily dosing schedule sufficient for achieving continual biomarker suppression with this agent.

In addition to schedule determination, we used these dose–response curves to determine pharmacodynamic biomarker-optimized doses for subsequent antitumor efficacy experiments. For each agent, we selected the final, optimized dose using clinically relevant dose increment ratios of 1.33 or 1.2, corresponding to a modified Fibonacci sequence (36, 37), to escalate from the dose level that had yielded slightly less than adequate $pY^{1234/1235}$MET/MET suppression. For EMD1214063, 10 mg/kg twice-daily yielded an average $pY^{1234/1235}$MET/MET suppression level slightly below the ≥90% suppression threshold at the 12-hour postdose time point, while 30 mg/kg twice daily maintained substantial $pY^{1234/1235}$MET/MET suppression (approximately 99%) at this time point (Fig. 2A); we therefore applied a standard 1.33 dose escalation increment to select for efficacy studies a dose of 12.5 mg/kg EMD1214063 twice daily. For XL880, $pY^{1234/1235}$MET/MET hovered very close to the 90% suppression threshold at the germane 24 hours postdose time point for the 14 mg/kg dose, but was suppressed well beyond this level for the 28 mg/kg dose; thus, we used the smallest clinically meaningful dose escalation increment (37), 1.2, to arrive at 17 mg/kg daily as the pharmacodynamics-optimized dosage regimen for XL880. In the case of XL184, the highest dose tested in our initial dose–pharmacodynamic response analysis, 33 mg/kg twice daily, did not yield sufficient biomarker suppression at 12-hour postdose (73% $pY^{1234/1235}$MET/MET suppression); we therefore used the standard 1.33 escalation increment, selecting a dose of 44 mg/kg twice-daily XL184 for efficacy testing.

Pharmacokinetic measurements are inadequate for predicting class-wide pharmacodynamic biomarker responses to MET TKIs

In replicating the design of a phase 0 study, we also analyzed tumor and plasma drug concentrations at selected time points for the highest dose tested for each agent to examine whether, as is often assumed in the clinic, these pharmacokinetic parameters serve as adequate surrogates for pharmacodynamic biomarker response. While $pY^{1234/1235}$MET/MET reduction was directly related to tumor and plasma drug exposure for EMD1214063,

Published OnlineFirst February 14, 2018; DOI: 10.1158/1535-7163.MCT-17-0552

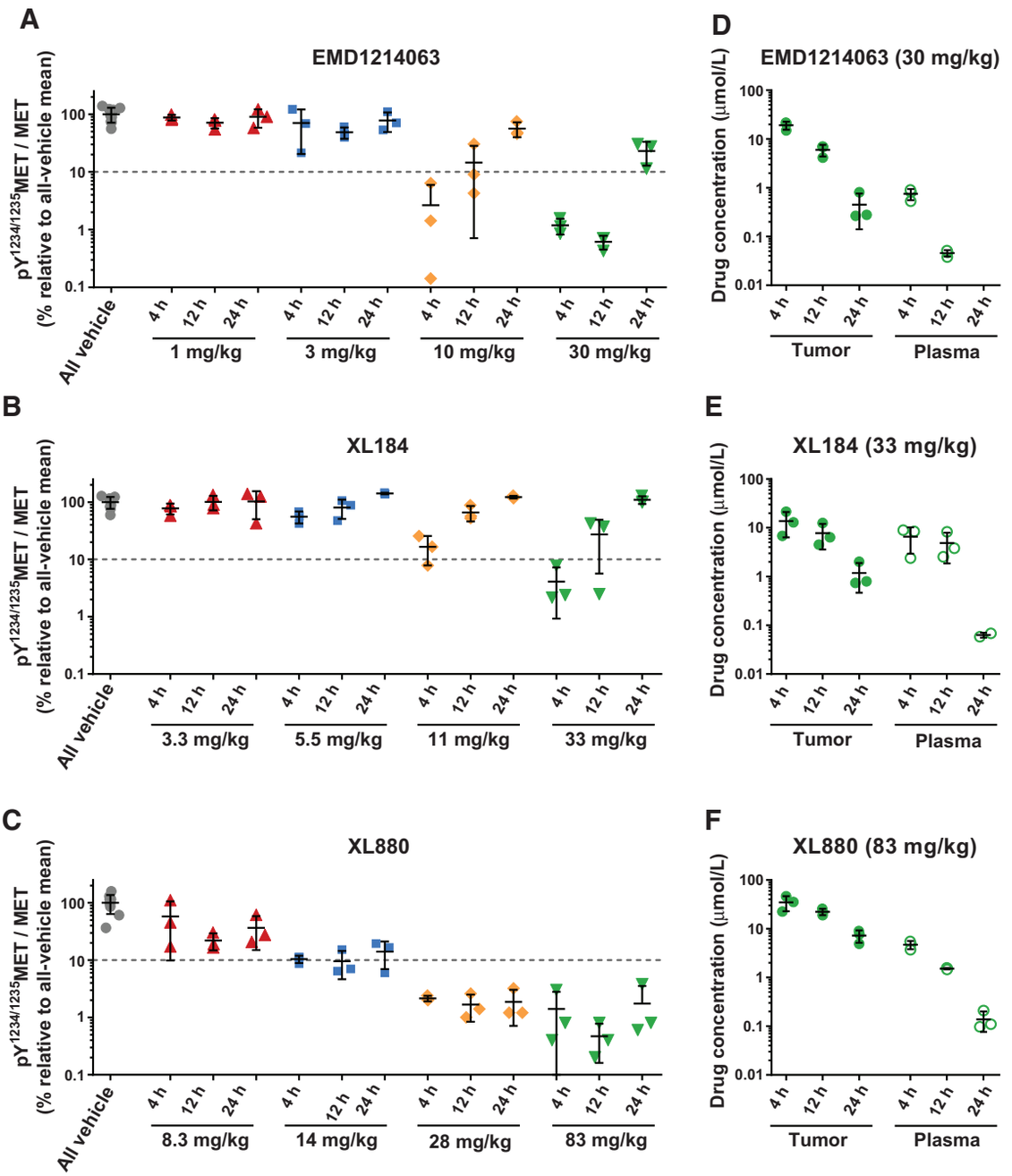

Figure 2.

Preclinical modeling of a phase 0 study indicates that MET kinase pharmacodynamic biomarker responses at 12 and 24 hours postdose are critical for determining MET inhibitor dosage regimens. **A–C,** $pY^{1234/1235}$MET/MET PD biomarker data (from Fig. 1) for the 4-, 12-, and 24-hour time points following administration of a single dose of EMD1214063 (**A**), XL184 (**B**), or XL880 (**C**), at the indicated dose levels, were selected to represent clinically feasible time points for sampling in a phase 0 study. The *y*-axis (log scale) indicates the pharmacodynamic biomarker value in each treated animal relative to the all-vehicle mean; the 90% inhibition threshold is indicated by the dotted line. **D–F,** Respective tumor and plasma pharmacokinetic data for these time points are shown for the highest doses of EMD1214063 (**D**), XL184 (**E**), and XL880 (**F**). In **D**, plasma EMD1214063 concentrations for all three samples at the 24-hour time point were below the lower limit of quantitation. For all panels, horizontal lines indicate the mean and SD for each group ($n = 3$ mice per group).

XL184, and XL880 (Fig. 2D–F), we found that the magnitudes of changes in these pharmacokinetic values did not reflect the pharmacodynamic biomarker response in a predictable fashion across even this small sample of MET TKIs [as might be expected on the basis of the differing chemical structures of these agents (Supplementary Fig. S1)]. For all three of these inhibitors, tumor

Published OnlineFirst February 14, 2018; DOI: 10.1158/1535-7163.MCT-17-0552

drug concentrations exceeded micromolar levels and were higher than the corresponding plasma concentrations (Fig. 2D–F; Supplementary Table S1). Furthermore, the time to maximum concentration was short (0.5–1.0 hours in plasma and 2–4 hours in tumor), indicating that all three agents were rapidly absorbed and distributed (Supplementary Table S2). In the case of EMD1214063, plasma and tumor drug concentrations decreased by 94% and 68%, respectively, between 4 and 12 hours postdose, while $pY^{1234/1235}$MET/MET decreased by 50% during this same time frame, indicating a lag between tumor penetration and pharmacodynamic biomarker response (Fig. 2A and D). In contrast, plasma and tumor levels of XL184 decreased by only 26% and 43%, respectively, from 4 to 12 hours postdose, while $pY^{1234/1235}$MET/MET increased by 5-fold during this time, suggesting rapid pharmacodynamic biomarker recovery for this agent even in the presence of substantial tumor drug concentrations (Fig. 2B and E). For XL880, $pY^{1234/1235}$MET/MET remained continually suppressed by over 98% at 4, 12, and 24 hours postdose despite the 79% and 97% reductions in plasma and tumor drug concentrations, respectively, from 4 to 24 hours, demonstrating a sustained pharmacodynamic biomarker response despite appreciable drug clearance (Fig. 2C and F). These variations in the relationships between pharmacodynamic biomarker response and both tumor and plasma drug concentrations demonstrate that, when selecting the optimal targeted agents and corresponding dosage regimens with which to treat patients, pharmacodynamic biomarker quantitation may represent a more direct method compared with traditional pharmacokinetic measurements.

Of note, the failure of ARQ197 to elicit a pharmacodynamic biomarker response at all dose levels tested (Fig. 1A; Supplementary Fig. S2A) occurred despite appreciable tumor drug concentrations (Supplementary Fig. S2B), so this agent was not evaluated further. For EMD1214063, XL184, and XL880, the pharmacodynamic biomarker–based dosage regimens described above were then used for antitumor efficacy comparisons among these agents.

Tumor regression achieved with customized, multi-day dosage regimens

Regression of SNU-5 xenograft tumors was achieved with the three MET inhibitors administered on a 21-day regimen (study days 18–38) using the customized doses and schedules that were predicted to continuously suppress $pY^{1234/1235}$MET/MET by 90% (Fig. 3). Robust tumor regression was apparent after only the fifth day of dosing for all 3 agents (study day 22) and was maintained throughout the duration of the dosing period (study days 18–38) and out to approximately study day 50, demonstrating the durability of tumor regression following treatment termination. Tumor weight was significantly different from vehicle control at every time point through the end of the study on day 62 ($P < 0.05$). Optimum %T/C values were 5 (day 46) for XL880, 0 (day 41) for XL184, and 6 (day 41) for EMD1214063, that is, at 8, 3, and 3 days, respectively, after the last dose of drug on day 38. There were no significant differences in antitumor efficacy among the inhibitors. Body weight did not differ significantly between drug- and vehicle-treated groups over the study period and did not exceed 3% loss in any animal (Supplementary Fig. S3), indicating that these pharmacodynamic-based dosage regimens produce sustained tumor regression at doses below those associated with substantial toxicity.

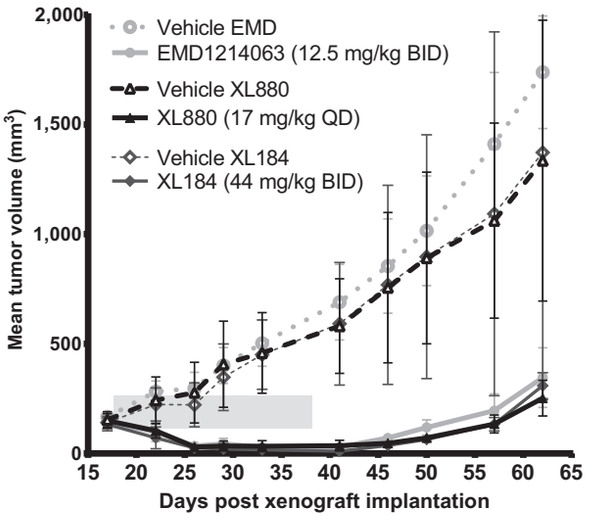

Figure 3.

Pharmacodynamic biomarker–based dosage regimens for XL880 (17 mg/kg once daily), XL184 (44 mg/kg twice daily), or EMD1214063 (12.5 mg/kg twice daily) yield equivalent tumor growth inhibition in the SNU-5 xenograft model. Drug dosing persisted for 21 days (shaded area), starting on study day 18 and continuing through day 38; mean tumor volumes were calculated to day 62. Significant growth inhibition relative to vehicle was measured for all three groups at all time points after day 18; tumor regression was observed from study day 22 through day 50, that is, beginning on the fifth day of treatment with each pharmacodynamics-guided dosage regimen. Error bars, SD ($n = 5$–16 animals per group).

Tumor pharmacodynamics of customized, multi-day dosage regimens

As predicted on the basis of our phase 0–like preclinical data, the customized doses and schedules that yielded tumor regression also maintained adequate $pY^{1234/1235}$MET/MET suppression throughout the entire duration of therapy. These regimens achieved average $pY^{1234/1235}$MET/MET PD biomarker reductions of 92%–99% at 4 hours after the first dose of each inhibitor ($P < 0.0001$ vs. mean of vehicle controls), and, similarly, of 95%–99% at 4 hours after the day 8 dose ($P < 0.0001$ vs. mean of vehicle controls; Fig. 4). For XL880, once-daily dosing achieved continuous suppression of $pY^{1234/1235}$MET/MET by > 92% both following single-dose treatment and throughout the eight-dose treatment, with biomarker suppression persisting at least 24 hours after treatment ended (Fig. 4A). For both XL184 and EMD1214063, the pharmacodynamic biomarker levels had returned to vehicle control levels by 24 hours after single-dose administration (Fig. 4B and C). However, in the XL184 and EMD1214063 multi-dose experiments (after withholding the day 8 afternoon doses scheduled by the twice-daily regimens), we observed that $pY^{1234/1235}$MET/MET remained suppressed by 88% and 95%, respectively, at 12 hours (i.e., precisely when the next dose was scheduled) but not at 24 hours following the final dose. These findings demonstrate the reversibility of MET kinase suppression as tumor drug levels fall, even after 8 days of drug treatment, as well as the key contribution of dose scheduling to continuous molecular target control.

Unexpectedly, both EMD1214063 and XL880 reduced levels of total full-length MET in addition to suppressing $pY^{1234/1235}$MET in the single-dose time course studies; total full-length MET levels

Published OnlineFirst February 14, 2018; DOI: 10.1158/1535-7163.MCT-17-0552

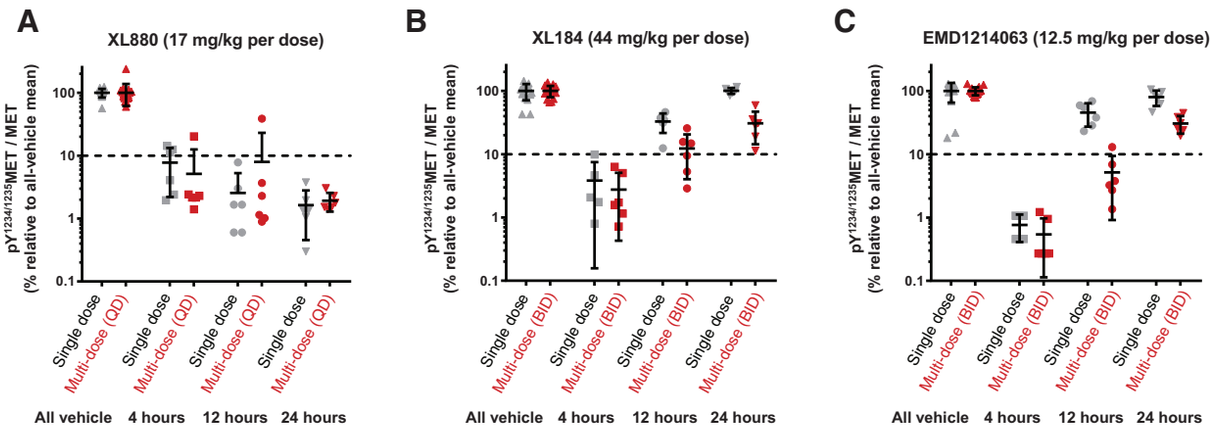

Figure 4.

Pharmacodynamic biomarker–based dosage regimens for XL880 (17 mg/kg once daily; **A**), XL184 (44 mg/kg twice daily; **B**), and EMD1214063 (12.5 mg/kg twice daily; **C**) maintain adequate $pY^{1234/1235}$MET/MET suppression in the SNU-5 xenograft model. Pharmacodynamic biomarker ($pY^{1234/1235}$MET/MET) levels relative to all-vehicle means are shown (on a log scale for clarity) at the indicated time points after dose 1 on treatment day 1 (gray) and either dose 8 for XL880 or dose 15 for XL184 and EMD1214063 on treatment day 8 (red). Note that the second doses of the day scheduled by the twice-daily regimens were withheld to characterize the response and recovery of the pharmacodynamic biomarker. The *y*-axis indicates the value of the pharmacodynamic biomarker, and the dotted line indicates the 90% pharmacodynamic biomarker suppression threshold. Horizontal lines indicate the mean and SD for each group ($n = 16$–18 for vehicle groups and $n = 4$–6 for all other groups).

were significantly reduced ($P < 0.05$) compared to the all-vehicle mean from 4 to 24 hours for the highest doses of EMD1214063 and from 24 to 48 hours for the highest doses of XL880 (Supplementary Fig. S4). Neither XL184 nor ARQ197 had a significant effect on total full-length MET levels at any time point after single-dose administration of any dose tested. In the multiple-dose studies using the PD-BEDRs, total full-length MET levels were 63%–85% lower than vehicle controls ($P < 0.001$) in all day 8 samples for all three TKIs (Supplementary Fig. S5). Declines in absolute MET levels would contribute to an increase in the value of the $pY^{1234/1235}$MET/MET biomarker, so the extensive drug suppression of the pharmacodynamic biomarker despite this backdrop of reduced MET levels indicates the effectiveness of the MET TKIs.

Further characterization of the pharmacodynamic–antitumor efficacy relationship for EMD1214063

To more precisely define the range of $pY^{1234/1235}$MET/MET levels associated with antitumor response to EMD1214063, we examined the single-dose pharmacodynamic biomarker response and corresponding multi-dose antitumor efficacy for doses above and below the PD-BEDR of 12.5 mg/kg twice-daily. To align our studies with the design of future clinical trials, we used EMD1214063 dose levels representing two consecutive 100% dose escalation increments (two trial cohorts) below and above the 12.5 mg/kg twice-daily dose level: 3.125 and 50 mg/kg twice-daily, respectively. We also compared the 50 mg/kg twice-daily regimen to the same dose administered on a once-daily schedule: 100 mg/kg once daily. As expected on the basis of the data shown in Fig. 1B, the single dose of 3.125 mg/kg did not achieve $\geq$ 90% $pY^{1234/1235}$MET/MET suppression at any time point tested, instead yielding an average $pY^{1234/1235}$MET/MET suppression of only approximately 50% at the relevant 12-hour time point (Fig. 5A; Table 1); when administered on a twice-daily schedule, the 3.125 mg/kg dose level yielded an average response of tumor growth stasis/slight regression during the treatment period, followed by regrowth after the cessation of drug administration (Fig. 5B), in contrast to the sustained tumor regression produced by our previously determined PD-BEDR of 12.5 mg/kg twice daily, which yielded an average $pY^{1234/1235}$MET/MET suppression of approximately 95% at 12 hours (Fig. 5A and B; Table 1). The 50 mg/kg twice-daily regimen resulted in $\geq$ 99% $pY^{1234/1235}$MET/MET suppression at 12 hours and an average antitumor response of sustained tumor regression that was not significantly different from that of the 12.5 mg/kg twice-daily group, confirming that doses exceeding the PD-BEDR do not provide additional gains in average antitumor activity (Fig. 5A and B; Table 1). However, the 100 mg/kg once-daily regimen likewise yielded $\geq$ 99% $pY^{1234/1235}$MET/MET suppression at the relevant 24-hour time point and sustained tumor regression, indicating that a daily dosing schedule is also capable of achieving a maximal antitumor response, albeit at an overall higher daily dose relative to the BID PD-BEDR. Importantly, the 100 mg/kg once-daily regimen, like all the other EMD1214063 regimens we tested, did not cause substantial reductions in body weight at any point during the experiment (Fig. 5C). Therefore, both the 12.5 mg/kg twice-daily and 100 mg/kg once-daily regimens represent optimized PD-BEDRs for EMD1214063.

We also determined the antitumor responses of individual animals using clinical RECIST (Response Evaluation Criteria in Solid Tumors) guidelines (38) to distinguish between progressive disease (PD; tumor volume increase of $\geq$20%), partial response (PR; tumor volume decrease of $\geq$ 30%), and stable disease (change in tumor volume between −30% and +20%) in comparisons of tumor volumes on the day prior to administration of the first dose (day 16) and the final experiment day (day 48). No animals in the 12.5 mg/kg twice-daily, 50 mg/kg twice-daily, or 100 mg/kg once-daily groups exhibited progressive disease, and no significant differences in the proportion of animals exhibiting SD versus PR were observed among these groups (according to Fisher exact test; Table 1), confirming that dosage regimens conferring sustained $pY^{1234/1235}$MET/MET suppression greater

Published OnlineFirst February 14, 2018; DOI: 10.1158/1535-7163.MCT-17-0552

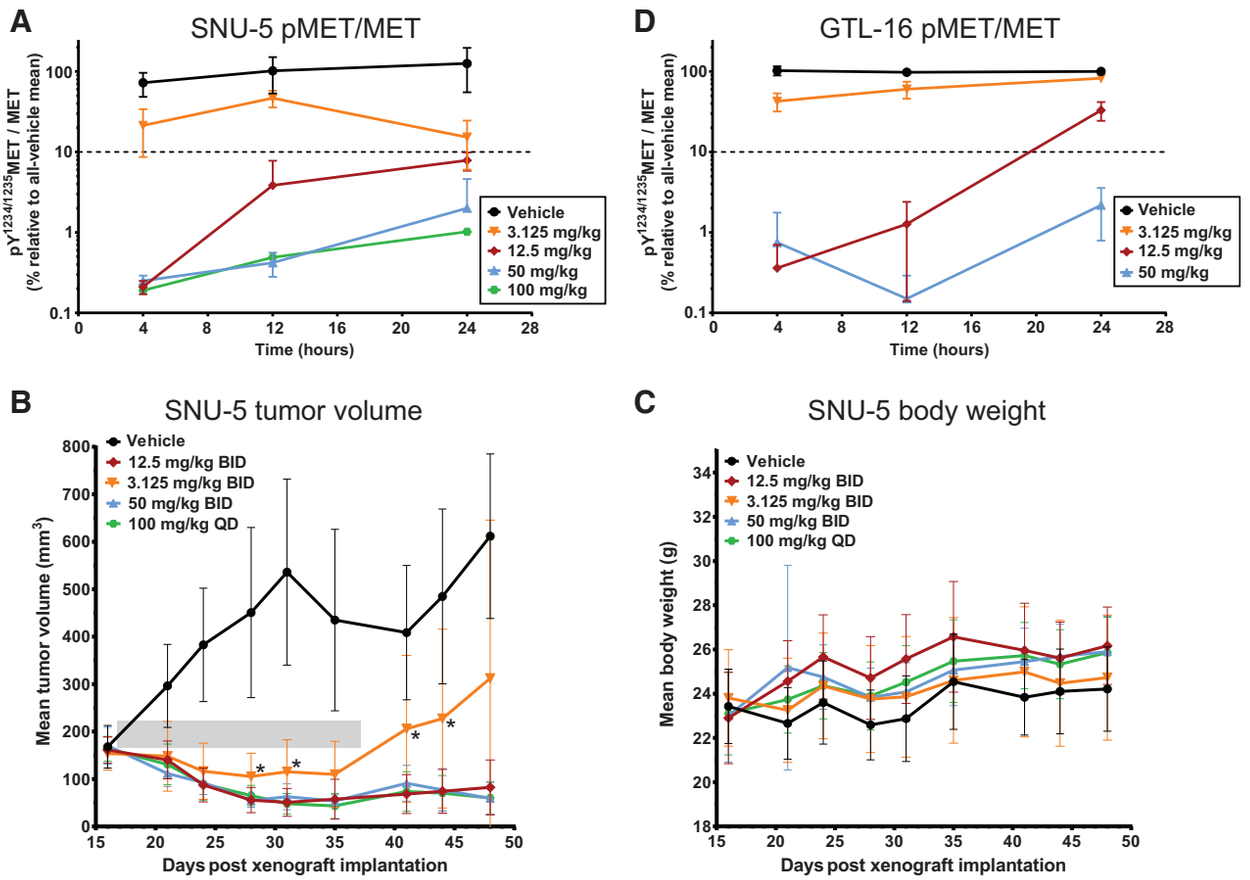

Figure 5.

Pharmacodynamic biomarker–based dosage regimen optimization defines $pY^{1234/1235}$MET/MET levels associated with transient or sustained EMD1214063-mediated tumor regression. **A** and **D,** Time course of $pY^{1234/1235}$MET/MET biomarker response to single-dose EMD1214063 at dose levels above and below the PD-BEDR dose (12.5 mg/kg) in the SNU-5 (**A**) and GTL-16 (**D**) xenograft models. The *x*-axis indicates time after drug administration, and the log-scale *y*-axis indicates the mean pharmacodynamic biomarker value in each group relative to the all-vehicle mean (90% inhibition threshold is indicated by the dotted line). Error bars represent SD ($n = 6$ animals per group). For samples in which the raw $pY^{1234/1235}$MET value was below the lower limit of quantitation (LLQ) for the assay, the LLQ value of 0.0016 fmol $pY^{1234/1235}$MET/μg total protein was used for calculating the mean biomarker response. **B,** Tumor growth in SNU-5 xenograft models treated with dosage regimens above and below the PD-BEDR for EMD1214063 (12.5 mg/kg twice-daily). Drug dosing with the indicated regimens persisted for 21 days (shaded box), starting on study day 17 and continuing through day 37; mean tumor volumes were calculated to day 48. Error bars represent SD ($n = 8$–10 animals per group), and asterisks indicate time points at which the mean tumor volume for the 3.125 mg/kg twice-daily group was significantly greater than that for the 12.5 mg/kg twice-daily group ($P < 0.05$ according to a two-tailed unpaired *t* test). **C,** EMD1214063 dosage regimens tested in **B** do not result in substantial animal body weight loss. Error bars, SD ($n = 8$–10 animals per group).

than the approximately 95% achieved by the previously defined PD-BEDR of 12.5 mg/kg twice-daily do not yield significantly improved antitumor responses. In contrast, the 3.125 mg/kg twice-daily regimen, which produced $pY^{1234/1235}$MET/MET suppression of approximately 50%, resulted in a significantly greater proportion of animals exhibiting progressive disease vs.

Table 1. Pharmacodynamic and antitumor response optimization for EMD1214063

Treatment group	$pY^{1234/1235}$MET/MET at relevant time point (%)[a]	Number of animals exhibiting given antitumor response[b]			
		PD	SD	PR	Total
Vehicle (BID)	101.9 ± 48.6	8	0	0	8
3.125 mg/kg BID	46.7 ± 10.9	5	1	4	10
12.5 mg/kg BID	3.8 ± 3.9	0	3	7	10
50 mg/kg BID	0.4 ± 0.1	0	1	9	10
100 mg/kg QD	1.0 ± 0.5	0	0	10	10

[a]Mean $pY^{1234/1235}$MET/MET values (± SD) for the time point at which next dose was scheduled to be administered in the given dosage regimen (12 hours for all groups except 100 mg/kg once daily, for which the response at 24 hours is shown). For pharmacodynamic data, $n = 6$ animals per group.

[b]PD, progressive disease; SD, stable disease; PR, partial response. Antitumor responses were designated according to RECIST criteria, comparing tumor volumes for each animal on the day prior to administration of the first dose versus last day of tumor measurement (days 16 vs. 48, respectively): PD, ≥ 20% tumor volume increase; PR, ≥ 30% reduction in tumor volume; SD, tumor volume change between −30% and +20%.

Published OnlineFirst February 14, 2018; DOI: 10.1158/1535-7163.MCT-17-0552

combined SD + PR (5 vs. 5 animals, respectively) relative to the 12.5 mg/kg twice-daily group (0 vs. 10 animals, respectively; $P = 0.03$ according to Fisher exact test; Table 1).

Finally, to assess the potential impact of xenograft model heterogeneity on the pharmacodynamic response to the EMD1214063 PD-BEDR, we measured the $pY^{1234/1235}$MET/MET response to single-dose EMD1214063 in an additional MET-driven model: the *MET*-amplified gastric carcinoma model GTL-16 (16). As in the SNU-5 model, we found that the 12.5 mg/kg and 50 mg/kg doses both yielded $pY^{1234/1235}$MET/MET suppression values of $\geq$90% at the relevant 12-hour time point in the GTL-16 model, while the 3.125 mg/kg dose resulted in an average $pY^{1234/1235}$MET/MET suppression of only 40% at 12 hours (Fig. 5D). These results, along with those from previous studies of the pMET suppression–efficacy relationship in the GTL-16 model (16, 17), indicate that the $pY^{1234/1235}$MET/MET–derived PD-BEDR for EMD1214063 established in the SNU-5 model is likely also applicable to other MET-driven models.

Discussion

Recognizing that clinical evaluation of molecularly targeted oncology agents at doses set by the MTD is suboptimal (2, 4, 39–41), we evaluated a clinically feasible, pharmacodynamically guided approach to identify biologically effective dosing regimens that would empirically link optimal target suppression with tumor regression in a relevant preclinical model, using MET TKIs as a test case. There are limited data comparing suppression of MET phosphorylation to antitumor efficacy; previous studies have found that > 90% transient reduction in MET phosphorylation corresponded to tumor growth inhibition, but not regression, in the *MET*-amplified GTL-16 and SNU-5 models (16, 17). One explanation for this treatment failure was target recovery during dosing intervals. We determined the extent of MET kinase inhibition (decreased $pY^{1234/1235}$MET/MET) during treatment of the *MET*-amplified SNU-5 gastric cancer xenograft model with ARQ197, XL880, XL184, or EMD121406. The time course and magnitude of $pY^{1234/1235}$MET/MET reduction varied considerably among MET inhibitors, so we defined the BED for each by identifying the minimal single dose required to achieve >90% reduction in tumor $pY^{1234/1235}$MET/MET, as well as the duration of that effect. Subsets of these data (comprised of measurements collected at a limited number of clinically feasible time points) were used to model a phase 0 study and demonstrate the translational potential of the PD-BEDR approach. Indeed, we used these "phase 0–like" data to identify the dose and schedule required to achieve sustained tumor $pY^{1234/1235}$MET/MET suppression and found that all of these pharmacodynamics-optimized dosage regimens were equally effective in achieving tumor regression in the SNU-5 xenograft model.

The PD-BEDRs we identified were well tolerated in terms of body weight loss, demonstrating that adequate molecular target control is sufficient for tumor regression and that this can be achieved at dose levels below those associated with toxicity. While mouse MTDs for the agents examined here are unknown, the total daily dose of each agent administered in the mouse PD-BEDR can be compared with both: (i) doses shown to be tolerable in previous mouse xenograft efficacy experiments and (ii) the mouse equivalent (42) of the human MTD (Supplementary Fig. S6). Both comparisons have caveats, including the lack of actual MTD determination in the former case and interspecies physiologic and biochemical differences in the latter. The total daily doses for XL880 and EMD1214063 PD-BEDRs are substantially lower than those shown to be tolerable in previous mouse xenograft efficacy studies (24, 27) and less than or equal to the mouse equivalents of the human MTDs for EMD1214063 and XL880, respectively (23, 43). In contrast, the total daily dose for the XL184 PD-BEDR is slightly greater than the highest dose shown to be tolerable in published xenograft studies (26) and approximately twice the mouse equivalent of the human MTD (22); thus, despite our data demonstrating no significant body weight loss from the XL184 PD-BEDR, rigorous toxicology analysis would be required to fully ensure tolerability of this regimen.

Despite the multitargeting nature of the MET TKIs examined here, our PD-BEDRs based exclusively on MET kinase inhibition conferred tumor regression in the SNU-5 xenograft model. SNU-5 gastric carcinoma cells are characterized by *MET* amplification, the absence of *MET* mutations, and constitutive, ligand-independent MET phosphorylation; these cells also undergo apoptosis upon MET signaling suppression (44). The similar dose–pharmacodynamic response relationship for EMD1214063 in the SNU-5 and GTL-16 models indicates that the $pY^{1234/1235}$MET/MET–based PD-BEDR we established for EMD1214063 in the SNU-5 model is likely also applicable to other *MET*-amplified, ligand-independent models. Whether or not our results would apply in ligand-dependent models, particularly those for which malignancy is driven by abnormalities in other kinase pathways, remains to be established. Both types of models do rely (at least in part) on MET signaling to drive proliferation, and MET inhibitors such as XL184 and EMD1214063 have exhibited antitumor activity in ligand-dependent and/or non-*MET*–amplified xenograft models (26, 27). However, for multikinase MET inhibitors such as XL184 and XL880, it is likely that dosage regimen optimization based exclusively on $pY^{1234/1235}$MET/MET will yield tumor regression only in cases where the activity of MET (rather than other kinase inhibitor targets) is the primary driver of malignancy.

Differences in the relationships between plasma and tumor drug concentrations and pMET inhibition were observed among the MET TKIs, emphasizing the importance of directly measuring MET kinase suppression rather than relying on plasma or tumor drug concentrations to estimate pharmacodynamic biomarker response. For example, for EMD1214063 and XL880, relatively stable tumor drug concentrations from 4 to 12 hours following single-dose administration maintained and gradually increased MET kinase suppression (Fig. 2). In contrast, relatively stable tumor concentrations of XL184 during the same time frame did not prevent recovery of MET kinase activity. This unique pharmacokinetic–pharmacodynamic relationship for XL184 could be explained by a steeper tumor concentration–biomarker response curve for XL184 compared with the other TKIs (perhaps due to XL184 binding and sequestration by other proteins within tumor tissue) or by compensatory mechanisms that increase levels of another XL184-binding protein, thereby reducing the effective concentration of free XL184. Alternatively, signaling crosstalk (45) could induce MET phosphorylation through other pathways (46, 47).

More generally, the uncoupling of target response and tumor and plasma drug concentrations indicates that reliance on plasma concentrations of targeted agents as surrogates for molecular target suppression in tumor could mislead dosage regimen determination. By directly measuring molecular target activity, pharmacodynamic biomarkers could play a critical role in optimizing

Published OnlineFirst February 14, 2018; DOI: 10.1158/1535-7163.MCT-17-0552

dosage regimens for continuous molecular target control and antitumor efficacy in diseases driven by that target. Use of pharmacodynamic data to complement, or even supplant, traditional, pharmacokinetics-guided dosage regimen optimization addresses the insufficiency of drug concentrations in surrogate tissues as accurate representations of target suppression levels in tumor (3).

ARQ197 failed to reduce $pY^{1234/1235}$MET/MET at any dose or time point examined, corroborating our previous findings (16). ARQ197 was originally reported as a highly selective, non-ATP–competitive MET inhibitor (48), and phase II results indicate that benefit from ARQ197 is limited to patients with high levels of total MET (49). However, recent *in vitro* studies have demonstrated that ARQ197-mediated cytotoxicity is independent of MET inhibition (34, 35) and may instead be due to effects on microtubule assembly (50, 51). Our studies provide the first *in vivo* evidence supporting these reports that ARQ197 is not a MET TKI.

Together with our previous analysis of the pharmacodynamic response of MET to targeted TKIs (16), our current findings highlight a critical role for validated pharmacodynamic marker assays in dosage regimen design: defining the range of between-dose biomarker recovery that does not compromise molecular target control and efficacy. Our previous findings in GTL-16 and SNU-5 xenograft models revealed that limiting pY^{1235}MET/MET recovery between doses to approximately 50% of baseline levels was sufficient for tumor growth stasis but not regression (16). Our current findings verify the lack of sustained tumor regression resulting from approximately 50% $pY^{1234/1235}$MET/MET suppression and indicate that limiting $pY^{1234/1235}$MET/MET recovery to $\leq$10% (i.e., $\geq$90% suppression) results in tumor regression in the SNU-5 model. We also further defined the window of biomarker suppression associated with tumor regression, finding that $pY^{1234/1235}$MET/MET suppression beyond approximately 90% does not confer additional gains in antitumor efficacy. The importance of limiting between-dose pMET recovery is corroborated by a previous study of EMD1214063, which found that 3 mg/kg daily dosing yielded substantial $pY^{1234/1235}$MET recovery within 24 hours (as measured by Western blotting) in the Hs746T *MET*-amplified gastric carcinoma model and was associated with tumor growth stasis only, while 6–10 mg/kg daily dosing yielded sustained $pY^{1234/1235}$MET suppression past the 24-hour time point and produced tumor regression (27). The authors also showed that once-daily dosing (50 mg/kg per dose) of another investigational MET inhibitor, EMD1204831, yielded tumor stasis in the EBC-1 *MET*–amplified non–small cell carcinoma model, while twice-daily dosing (25 mg/kg per dose) of this agent (which was hypothesized to better maintain $pY^{1234/1235}$MET suppression) yielded partial tumor regression. In this study, we identified both once-daily and twice-daily regimens of EMD1214063 (100 mg/kg once-daily and 12.5 mg/kg twice-daily) that yielded sustained $\geq$ 90% $pY^{1234/1235}$MET/MET suppression and tumor regression in the SNU-5 model, illustrating the importance of considering both dose and schedule in dosage regimen optimization; this knowledge of both once- and twice-daily PD-BEDRs may prove particularly valuable when developing novel combination therapies.

These findings may be readily translated into establishing PD-BEDRs in the clinic. Estimating profiles of pharmacodynamic biomarker response recovery and associated tumor control in preclinical models, as we have accomplished here for MET TKIs, should help optimize dosage regimens for other classes of targeted agents. Clinically, dosage regimens could be optimized and evaluated in a phase 0 trial, as we have modeled here in a preclinical setting using our validated, clinically suitable (52) pMET assay. Results from a phase 0 trial comparing the pharmacodynamic biomarker responses to several agents would inform subsequent phase I/II trials comparing safety and efficacy of the optimized, BED-based schedule for each drug. Only inhibitors capable of reducing target activity levels to the predefined threshold in the phase 0 study would advance to phase I/II trials, either as single agents or in combination therapies to address drug resistance issues.

Results of a recent XL184 trial underscore the clinical significance of directly measuring MET kinase suppression to reduce toxicities while maintaining or even improving the efficacies of MET inhibitor therapeutic regimens. In this phase III trial of XL184 in metastatic medullary thyroid cancer, 79% of patients required dose reductions as a result of adverse events following a 140-mg once-daily regimen (53). To address this issue, a dose-comparison trial to assess the efficacy of a lower XL184 dose is currently underway (clinicaltrials.gov identifier: NCT01896479). Application of the PD-BEDR approach in a phase 0 trial of XL184 might have enabled determination of a dosage regimen that maintains optimal MET kinase suppression while avoiding such tolerability issues.

Our findings point to pharmacodynamics-guided scheduling of biologically effective doses as a key aspect of targeted agent development. Customary pharmacodynamic studies typically include only a single "snapshot" of target response to drug at a predetermined time point after drug administration. Our work demonstrates the value of a more detailed characterization of the dynamics of pharmacodynamic response to targeted agents and suggests that clinical pharmacodynamic studies may be missing critical drug development information if the protocol prescribes the same time point for evaluation in all patients. The MET TKIs studied here represent different chemical families (Supplementary Fig. S1) and display different kinase profiles (24, 26, 27), yet when administered optimally in the SNU-5 model, none could be considered superior. Clinically, this suggests that a compound will deserve "best-in-class" designation because it is practical to administer its optimized PD-BEDR, and it is well tolerated. The objective of our current study was not to identify the best-in-class preclinical agent but to evaluate use of $pY^{1234/1235}$MET/MET as a pharmacodynamic biomarker of MET inhibitor response and its value in providing pharmacodynamic guidance to establish optimal dosage regimens for development of MET inhibitors. We foresee the application of this approach to other therapeutic classes of molecularly targeted agents.

Disclosure of Potential Conflicts of Interest

No potential conflicts of interest were disclosed.

Authors' Contributions

Conception and design: A.K. Srivastava, M.G. Hollingshead, J.M. Covey, M.A. Simpson, R.J. Kinders, J.H. Doroshow, R.E. Parchment

Development of methodology: A.K. Srivastava, M.A. Simpson, J.J. Wright

Acquisition of data (provided animals, acquired and managed patients, provided facilities, etc.): A.K. Srivastava, M.G. Hollingshead, J.P. Govindharajulu, D.P. Bottaro

Analysis and interpretation of data (e.g., statistical analysis, biostatistics, computational analysis): A.K. Srivastava, J.P. Govindharajulu, J.M. Covey, D. Liston, J.O. Peggins, D.P. Bottaro, J.H. Doroshow, R.E. Parchment

Writing, review, and/or revision of the manuscript: A.K. Srivastava, J.M. Covey, M.A. Simpson, J.O. Peggins, D.P. Bottaro, J.J. Wright, J.H. Doroshow, R.E. Parchment

Administrative, technical, or material support (i.e., reporting or organizing data, constructing databases): A.K. Srivastava, J.P. Govindharajulu, J.H. Doroshow
Study supervision: A.K. Srivastava, M.G. Hollingshead, R.J. Kinders, R.E. Parchment
Other (provided clinical context): J.J. Wright

Acknowledgments

This project has been funded in whole or in part with federal funds from the National Cancer Institute, NIH, under contract no. HHSN261200800001E. The content of this publication does not necessarily reflect the views or policies of the Department of Health and Human Services, nor does mention of trade names, commercial products, or organizations imply endorsement by the U.S. Government. The authors wish to thank NCI contract investigators at SRI International (HHSN261201100012C), Southern Research Institute (HHSN261201100013C), and the University of California-San Francisco (HHSN261201100016C) for determination of plasma and tumor compound levels. The authors thank Jennifer Weiner, and Suzanne Borgel, Carrie Bonomi, John Carter, Raymond Divelbiss, Howard Stotler, and Michelle Gottholm-Ahalt for excellent technical support conducting the validated pharmacodynamic assay and the preclinical animal studies, respectively. The authors thank Dr. Joel Morris for the drawing of the chemical structures of the MET inhibitors and Drs. Andrea Regier Voth, Leidos Biomedical Research, Inc., and Sarah Miller, Kelly Services, for editorial support in the preparation of this manuscript.

The costs of publication of this article were defrayed in part by the payment of page charges. This article must therefore be hereby marked *advertisement* in accordance with 18 U.S.C. Section 1734 solely to indicate this fact.

Received June 21, 2017; revised December 11, 2017; accepted December 29, 2017; published OnlineFirst February 14, 2018.

References

1. Bullock JM, Rahman A, Liu Q. Lessons learned: dose selection of small molecule–targeted oncology drugs. Clin Cancer Res 2016;22:2630–8.
2. Sachs JR, Mayawala K, Gadamsetty S, Kang SP, de Alwis DP. Optimal dosing for targeted therapies in oncology: drug development cases leading by example. Clin Cancer Res 2016;22:1318–24.
3. Parchment RE, Doroshow JH. Pharmacodynamic endpoints as clinical trial objectives to answer important questions in oncology drug development. Semin Oncol 2016;43:514–25.
4. Postel-Vinay S, Arkenau HT, Olmos D, Ang J, Barriuso J, Ashley S, et al. Clinical benefit in Phase-I trials of novel molecularly targeted agents: does dose matter? Br J Cancer 2009;100:1373–8.
5. Turnidge JD. The pharmacodynamics of beta-lactams. Clin Infect Dis 1998;27:10–22.
6. Murgo AJ, Kummar S, Rubinstein L, Gutierrez M, Collins J, Kinders R, et al. Designing phase 0 cancer clinical trials. Clin Cancer Res 2008;14:3675–82.
7. Kummar S, Kinders R, Gutierrez ME, Rubinstein L, Parchment RE, Phillips LR, et al. Phase 0 clinical trial of the poly (ADP-ribose) polymerase inhibitor ABT-888 in patients with advanced malignancies. J Clin Oncol 2009;27:2705–11.
8. LoRusso PM, Li J, Burger A, Heilbrun LK, Sausville EA, Boerner SA, et al. Phase I safety, pharmacokinetic, and pharmacodynamic study of the poly (ADP-ribose) polymerase (PARP) inhibitor veliparib (ABT-888) in combination with irinotecan in patients with advanced solid tumors. Clin Cancer Res 2016;22:3227–37.
9. Kummar S, Ji J, Morgan R, Lenz HJ, Puhalla SL, Belani CP, et al. A phase I study of veliparib in combination with metronomic cyclophosphamide in adults with refractory solid tumors and lymphomas. Clin Cancer Res 2012;18:1726–34.
10. Reiss KA, Herman JM, Zahurak M, Brade A, Dawson LA, Scardina A, et al. A Phase I study of veliparib (ABT-888) in combination with low-dose fractionated whole abdominal radiation therapy in patients with advanced solid malignancies and peritoneal carcinomatosis. Clin Cancer Res 2015;21:68–76.
11. Peters S, Adjei AA. MET: a promising anticancer therapeutic target. Nat Rev Clin Oncol 2012;9:314–26.
12. Trusolino L, Bertotti A, Comoglio PM. MET signalling: principles and functions in development, organ regeneration and cancer. Nat Rev Mol Cell Biol 2010;11:834–48.
13. Eder JP, Vande Woude GF, Boerner SA, LoRusso PM. Novel therapeutic inhibitors of the c-Met signaling pathway in cancer. Clin Cancer Res 2009;15:2207–14.
14. Zhu H, Naujokas MA, Fixman ED, Torossian K, Park M. Tyrosine 1356 in the carboxyl-terminal tail of the HGF/SF receptor is essential for the transduction of signals for cell motility and morphogenesis. J Biol Chem 1994;269:29943–8.
15. Chiara F, Michieli P, Pugliese L, Comoglio PM. Mutations in the met oncogene unveil a "dual switch" mechanism controlling tyrosine kinase activity. J Biol Chem 2003;278:29352–8.
16. Srivastava AK, Hollingshead MG, Weiner J, Navas T, Evrard YA, Khin SA, et al. Pharmacodynamic response of the MET/HGF-receptor to small molecule tyrosine kinase inhibitors examined with validated, fit-for-clinic immunoassays. Clin Cancer Res 2016;22:3683–94.
17. Yamazaki S, Skaptason J, Romero D, Lee JH, Zou HY, Christensen JG, et al. Pharmacokinetic-pharmacodynamic modeling of biomarker response and tumor growth inhibition to an orally available cMet kinase inhibitor in human tumor xenograft mouse models. Drug Metab Dispos 2008; 36:1267–74.
18. Zou HY, Li Q, Lee JH, Arango ME, McDonnell SR, Yamazaki S, et al. An orally available small-molecule inhibitor of c-Met, PF-2341066, exhibits cytoreductive antitumor efficacy through antiproliferative and antiangiogenic mechanisms. Cancer Res 2007;67:4408–17.
19. Yamazaki S. Translational pharmacokinetic-pharmacodynamic modeling from nonclinical to clinical development: a case study of anticancer drug, crizotinib. AAPS J 2013;15:354–66.
20. Eder JP, Shapiro GI, Appleman LJ, Zhu AX, Miles D, Keer H, et al. A phase I study of foretinib, a multi-targeted inhibitor of c-Met and vascular endothelial growth factor receptor 2. Clin Cancer Res 2010;16:3507–16.
21. Yap TA, Olmos D, Brunetto AT, Tunariu N, Barriuso J, Riisnaes R, et al. Phase I trial of a selective c-MET inhibitor ARQ 197 incorporating proof of mechanism pharmacodynamic studies. J Clin Oncol 2011;29:1271–9.
22. Kurzrock R, Sherman SI, Ball DW, Forastiere AA, Cohen RB, Mehra R, et al. Activity of XL184 (Cabozantinib), an oral tyrosine kinase inhibitor, in patients with medullary thyroid cancer. J Clin Oncol 2011;29:2660–6.
23. Falchook GS, Kurzrock R, Amin HM, Fu S, Piha-Paul SA, Janku F, et al. Efficacy, safety, biomarkers, and phase II dose modeling in a phase I trial of the oral selective c-Met inhibitor tepotinib (MSC2156119J). J Clin Oncol 2015;33:2591.
24. Qian F, Engst S, Yamaguchi K, Yu P, Won KA, Mock L, et al. Inhibition of tumor cell growth, invasion, and metastasis by EXEL-2880 (XL880, GSK1363089), a novel inhibitor of HGF and VEGF receptor tyrosine kinases. Cancer Res 2009;69:8009–16.
25. Traynor K. Cabozantinib approved for advanced medullary thyroid cancer. Am J Health Syst Pharm 2013;70:88.
26. Yakes FM, Chen J, Tan J, Yamaguchi K, Shi Y, Yu P, et al. Cabozantinib (XL184), a novel MET and VEGFR2 inhibitor, simultaneously suppresses metastasis, angiogenesis, and tumor growth. Mol Cancer Ther 2011;10: 2298–308.
27. Bladt F, Faden B, Friese-Hamim M, Knuehl C, Wilm C, Fittschen C, et al. EMD 1214063 and EMD 1204831 constitute a new class of potent and highly selective c-Met inhibitors. Clin Cancer Res 2013;19:2941–51.
28. Adjei AA, Schwartz B, Garmey E. Early clinical development of ARQ 197, a selective, non–ATP-competitive inhibitor targeting MET tyrosine kinase for the treatment of advanced cancers. Oncologist 2011;16:788–99.
29. Smith DC, Smith MR, Sweeney C, Elfiky AA, Logothetis C, Corn PG, et al. Cabozantinib in patients with advanced prostate cancer: results of a phase II randomized discontinuation trial. J Clin Oncol 2013;31:412–9.
30. Medová M, Pochon B, Streit B, Blank-Liss W, Francica P, Stroka D, et al. The novel ATP-competitive inhibitor of the MET hepatocyte growth factor receptor EMD1214063 displays inhibitory activity against selected MET-mutated variants. Mol Cancer Ther 2013;12:2415–24.

31. Hollingshead MG. Antitumor efficacy testing in rodents. J Natl Cancer Inst 2008;100:1500–10.
32. Pfister TD, Hollingshead M, Kinders RJ, Zhang Y, Evrard YA, Ji J, et al. Development and validation of an immunoassay for quantification of topoisomerase I in solid tumor tissues. PLoS One 2012;7:e50494.
33. Kinders RJ, Hollingshead M, Khin S, Rubinstein L, Tomaszewski JE, Doroshow JH, et al. Preclinical modeling of a phase 0 clinical trial: qualification of a pharmacodynamic assay of poly (ADP-ribose) polymerase in tumor biopsies of mouse xenografts. Clin Cancer Res 2008;14: 6877–85.
34. Basilico C, Pennacchietti S, Vigna E, Chiriaco C, Arena S, Bardelli A, et al. Tivantinib (ARQ197) displays cytotoxic activity that is independent of its ability to bind MET. Clin Cancer Res 2013;19:2381–92.
35. Calles A, Kwiatkowski N, Cammarata BK, Ercan D, Gray NS, Janne PA. Tivantinib (ARQ 197) efficacy is independent of MET inhibition in non-small-cell lung cancer cell lines. Mol Oncol 2015;9:260–9.
36. Penel N, Kramar A. What does a modified-Fibonacci dose-escalation actually correspond to? BMC Med Res Methodol 2012;12:103.
37. Konner JA, O'Reilly EM. Clinical trial design and methodology. In:Von Hoff DD, Evans DB, andHruban RH, editors. Pancreatic cancer. Boston, MA: Jones and Bartlett; 2005. p.466.
38. Eisenhauer EA, Therasse P, Bogaerts J, Schwartz LH, Sargent D, Ford R, et al. New response evaluation criteria in solid tumours: revised RECIST guideline (version 1.1). Eur J Cancer 2009;45:228–47.
39. Goulart BH, Clark JW, Pien HH, Roberts TG, Finkelstein SN, Chabner BA. Trends in the use and role of biomarkers in phase I oncology trials. Clin Cancer Res 2007;13:6719–26.
40. Gutierrez ME, Kummar S, Giaccone G. Next generation oncology drug development: opportunities and challenges. Nat Rev Clin Oncol 2009; 6:259–65.
41. Parchment RE, Doroshow JH. Theory and practice of clinical pharmacodynamics in oncology drug development. Semin Oncol 2016;43:427–35.
42. Nair AB, Jacob S. A simple practice guide for dose conversion between animals and human. J Basic Clin Pharm 2016;7:27–31.
43. Shapiro GI, McCallum S, Adams LM, Sherman L, Weller S, Swann S, et al. A Phase 1 dose-escalation study of the safety and pharmacokinetics of once-daily oral foretinib, a multi-kinase inhibitor, in patients with solid tumors. Invest New Drugs 2013;31:742–50.
44. Smolen GA, Sordella R, Muir B, Mohapatra G, Barmettler A, Archibald H, et al. Amplification of MET may identify a subset of cancers with extreme sensitivity to the selective tyrosine kinase inhibitor PHA-665752. Proc Natl Acad Sci U S A 2006;103:2316–21.
45. Organ SL, Tsao MS. An overview of the c-MET signaling pathway. Ther Adv Med Oncol 2011;3:S7–S19.
46. Dulak AM, Gubish CT, Stabile LP, Henry C, Siegfried JM. HGF-independent potentiation of EGFR action by c-Met. Oncogene 2011;30:3625–35.
47. Varkaris A, Gaur S, Parikh NU, Song JH, Dayyani F, Jin JK, et al. Ligand-independent activation of MET through IGF-1/IGF-1R signaling. Int J Cancer 2013;133:1536–46.
48. Eathiraj S, Palma R, Volckova E, Hirschi M, France DS, Ashwell MA, et al. Discovery of a novel mode of protein kinase inhibition characterized by the mechanism of inhibition of human mesenchymal-epithelial transition factor (c-Met) protein autophosphorylation by ARQ 197. J Biol Chem 2011;286:20666–76.
49. Santoro A, Rimassa L, Borbath I, Daniele B, Salvagni S, Van Laethem JL, et al. Tivantinib for second-line treatment of advanced hepatocellular carcinoma: a randomised, placebo-controlled phase 2 study. Lancet Oncol 2013;14:55–63.
50. Aoyama A, Katayama R, Oh-Hara T, Sato S, Okuno Y, Fujita N. Tivantinib (ARQ 197) exhibits antitumor activity by directly interacting with tubulin and overcomes ABC transporter-mediated drug resistance. Mol Cancer Ther 2014;13:2978–90.
51. Katayama R, Aoyama A, Yamori T, Qi J, Oh-hara T, Song Y, et al. Cytotoxic activity of tivantinib (ARQ 197) is not due solely to c-MET inhibition. Cancer Res 2013;73:3087–96.
52. Srivastava AK, Govindharajulu JP, Park SR, Navas T, Ferry-Galow KV, Kinders RJ, et al. Pazopanib to suppress MET signaling in patients with refractory advanced solid tumors [abstract]. J Clin Oncol 34:15s, 2016 (suppl; abstr 2553).
53. Elisei R, Schlumberger MJ, Müller SP, Schöffski P, Brose MS, Shah MH, et al. Cabozantinib in progressive medullary thyroid cancer. J Clin Oncol 2013;31:3639–46.

Published OnlineFirst February 14, 2018; DOI: 10.1158/1535-7163.MCT-17-0552

Molecular Cancer Therapeutics

Molecular Pharmacodynamics-Guided Scheduling of Biologically Effective Doses: A Drug Development Paradigm Applied to MET Tyrosine Kinase Inhibitors

Apurva K. Srivastava, Melinda G. Hollingshead, Jeevan Prasaad Govindharajulu, et al.

Mol Cancer Ther 2018;17:698-709. Published OnlineFirst February 14, 2018.